NEW PARAMETER ESTIMATION APPROACHES FOR DUAL-INPUT ^{11}C-ACETATE LIVER KINETIC MODEL

Sirong Chen[1], Dagan Feng[1, 2]

1. *Center for Multimedia Signal Processing, Department of Electronic and Information Engineering, The Hong Kong Polytechnic University, Hong Kong,*
2. *Biomedical and Multimedia Information Technology Group, School of Information Technologies, The University of Sydney, Australia.*

Abstract: ^{11}C-acetate uptake in hepatocellular carcinoma (HCC) was reported and the modeling study has been conducted, in which the weighted nonlinear least squares (NLS) algorithm was used to estimate all of the parameters. However, the computational time-complexity of NLS method is high and some estimates are not quite reliable. Due to the hepatic dual blood supply, the current developed fast algorithms could not be used directly. In this paper, two new estimation approaches were presented: Patlak-NLS and Patlak-dual-input-generalized linear least squares. The estimation results demonstrated that these two methods could provide better and practical ways for dual-input ^{11}C-acetate liver kinetic modeling.

Keywords: Algorithms, Biomedical systems, Dual-input, Model, Parameter estimation.

1. INTRODUCTION

Application of the tracer kinetic modeling technique in positron emission tomography (PET) could provide significant diagnostic information for various kinds of disease detection. Quantitative PET using labeled ^{11}C-acetate provides the ability to evaluate non-^{18}F-fluorodeoxyglucose (FDG)-avid hepatocellular carcinoma (HCC) (Ho, *et al.*, 2003; Chen, *et al.*, 2004; Chen and Feng, 2004), a highly malignant tumor. A three-compartment model describing ^{11}C-acetate liver kinetics with an extra parameter (relative portal venous contribution to the hepatic blood supply) included in the model input function to account for the dual source of liver blood supply has been proposed and validated by Chen and Feng (2004). In the previous modeling studies, all of the parameters were estimated by using the weighted nonlinear least squares (NLS) algorithm. However, due to the relative large number of parameters to be estimated, the computational time-complexity is high, the fitting results are a bit more sensitive to the initial guess, and some estimates are not quite reliable, which limits its routing application in the clinical environments.

With the development of high spatial and temporal resolution PET, a variety of rapid parameter estimation methodologies have been developed (Huang, *et al.*, 1982; Patlak, *et al.*, 1983; Carson, *et al.*, 1986; Feng, *et al.*, 1996; Chen, *et al.*, 1998). All these computationally efficient techniques are to identify single input systems, and could not provide solutions for dual-input biomedical systems directly. Therefore, practical algorithms are needed to be developed for the parameter estimation of dual-input ^{11}C-acetate liver kinetic model to detect HCC.

In this study, two novel parameter estimation approaches for ^{11}C-acetate kinetic model of dual-input liver system were presented: Patlak-NLS and Patlak- dual-input-generalized linear least squares (Patlak-D-I-GLLS) algorithms. The performance in terms of the estimation reliability and accuracy of Patlak-NLS and Patlak-D-I-GLLS techniques were

evaluated by the clinical datasets and computer simulation respectively.

2. METHODS

2.1 Human studies.

The study population comprised six subjects with two suffered from HCC. Dynamic PET images were recorded for 10 min after injection of ^{11}C-acetate as 25 frames with the following scan durations: 10×4, 8×10, 2×30, 3×60 and 2×120 sec. Time-activity curve (TAC) was generated by placing a region of interest (ROI) on single transverse slice of the full set of dynamic PET images. Eight ROIs were extracted from nontumor liver tissue of the six patients and two HCC regions were extracted from the two patients suffered from HCC. The TAC in blood (BTAC) consisting of the hepatic artery (HA) and portal vein (PV), whose TACs were image derived, was used as the model input function. As suggested by Munk *et al.* (2001) that after some time the TACs of HA and PV are virtually identical, to avoid the radioactivity spillover from the surrounding tissue to the PV, the last five measurements of the PV were replaced by the corresponding HA data in this study.

2.2 ^{11}C-acetate kinetic model in liver.

The dual-input ^{11}C-acetate liver kinetic model was proposed by Chen and Feng (2004), which consists of three compartments (Fig. 1), corresponding to the intravascular ^{11}C-acetate concentration, the intracellular free ^{11}C-acetate and the intracellular ^{11}C-acetate products/metabolites converted from ^{11}C-acetate (acetyl-CoA, and metabolites of fatty acid synthesis). *HBV* (hepatic blood volume) is to account for the contribution of ^{11}C-acetate within vascular/sinus space of liver tissue to the observed total tissue activity. The differential equations describing the kinetics of ^{11}C-acetate in liver are given by

$$\frac{d}{dt}c_e(t) = K_1 c_b(t) - (k_2 + k_3)c_e(t) \quad (1)$$

$$\frac{d}{dt}c_m(t) = k_3 c_e(t) \quad (2)$$

$$c_i(t) = c_e(t) + c_m(t) \quad (3)$$

where K_1-k_3 are the rate constants, $c_b(t)$ and $c_e(t)$ are the ^{11}C-acetate concentration in intravascular and intracellular space respectively, $c_m(t)$ is the intracellular products/metabolites concentration. The observed total tissue activity $c_T(t)$, is given by

$$c_T(t) = c_i(t) + HBV * c_b(t) \quad (4).$$

The dual-input function $c_b(t)$ is calculated by

$$c_b(t) = (1 - a_v) * c_a(t) + a_v * c_v(t) \quad (5)$$

where $c_a(t)$ and $c_v(t)$ are the tracer concentration in the HA and PV respectively, and a_v is to account for the relative portal venous contribution to the hepatic blood supply.

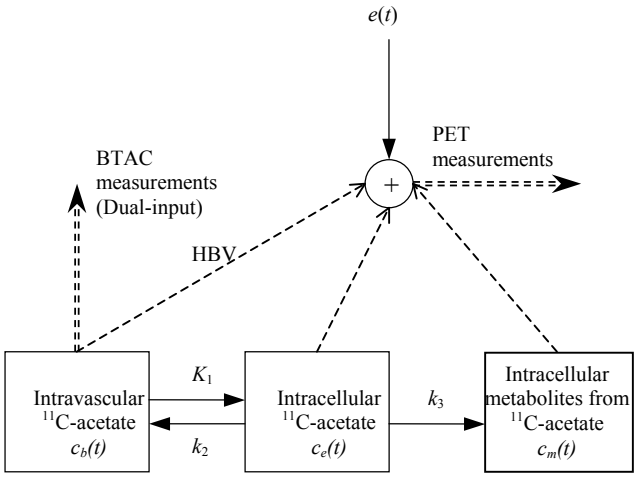

Fig. 1. The three-compartment ^{11}C-acetate liver kinetic model with the dual-input function. *e(t)* denotes the PET measurement noise.

2.3 Patlak-nonlinear least squares algorithm.

The parameter estimation procedure of this Patlak-NLS technique has the following three steps.

1. Linear Patlak method is applied to estimate the HCC indicator "local hepatic metabolic rate-constant of acetate (LHMRAct)" formulated as $K_1*k_3/(k_2+k_3)$ (the forward clearance *K*) (Chen, *et al.*, 2004; Chen and Feng, 2004). The data to be fitted are from 3 min to 10 min, when the two TACs of HA and PV are almost virtually identical. To calculate the dual-input function, a_v was fixed as 0.8 for the first iteration.
2. Since $K_1*k_3/(k_2+k_3)$ is one of the macro-parameters of the ^{11}C-acetate model, the weighted NLS algorithm is utilized to estimate *HBV*, a_v and the other two macroparameters: $K_1*k_2/(k_2+k_3)$ and (k_2+k_3). This fitting procedure is to minimize the weighted residual sum of squares (WRSS). The weights used are proportional to the frame duration divided by the concentration value of that time point. If the difference between the estimated a_v by this NLS regression and the a_v value utilized in step 1 is greater than 0.2, which may generally indicate the tumor case, steps 1 and 2 would be performed again. The estimated a_v would be used to calculate the dual-input function in step 1. For nontumor cases, the iteration generally would not be repeated since the a_v value obtained by the previous quantitative study (Chen and Feng, 2004) is 0.7935 ± 0.1040; for tumor cases, one more iteration is generally needed.
3. Parameter *K* would be estimated by Patlak method with the updated a_v value in step 2 to calculate the dual-input function.

The fitting results by Patlak-NLS approach were compared with those obtained from NLS method. The coefficient of variation (*CV*) was adopted as the statistical criterion to access the reliability of the parameter estimation.

2.4 Patlak-dual-input-generalized linear least squares algorithm.

The Patlak-D-I-GLLS technique is a novel fast estimation algorithm consisting of four steps. The first step estimation is the same as that involved in the Patlak-NLS algorithm. The second step estimation is Patlak-dual-input-linear least squares (Patlak-D-I-LLS) proposed in this paper. The second-order differential equation of the ^{11}C-acetate liver kinetic model could be expressed as

$$c_T^{''}(t) = HBV * c_b^{''}(t) + \left[K_1 + (k_2 + k_3)HBV\right] * c_b^{'}(t) + K_1 k_3 * c_b(t) - (k_2 + k_3) * c_T^{'}(t) \quad (6).$$

Substitute K_1k_3 in eq. (6) by $\hat{K}(k_2 + k_3)$, where $\hat{K}$ is the estimation value in step one. Let P_0=HBV, P_1=K_1+(k_2+k_3)HBV, and P_2=k_2+k_3, then,

$$c_T^{''}(t) = P_0 * c_b^{''}(t) + P_1 * c_b^{'}(t) + \hat{K}P_2 * c_b(t) - P_2 * c_T^{'}(t) \quad (7).$$

To formulate the Patlak-D-I-LLS solution, substitute $c_b(t)$ in the first term of eq. (7) with eq. (5) and assume the initial conditions were all zeros, the observed total tissue activity $c_T(t)$, is

$$c_T(t) = P_0 * c_a(t) + P_3(c_v(t) - c_a(t)) + P_1\int_0^t c_b(\tau)d\tau + \hat{K}P_2\int_0^t\int_0^t c_b(\tau)d\tau^2 - P_2\int_0^t c_T(\tau)d\tau \quad (8)$$

where P_3=HBV*a_v. Digitalize eq. (8) at the sampling time t_0, t_1, … , and t_m, and include the equation noise ξ , the linear equation in matrix form is

$$y = X\theta + \xi \quad (9)$$

where y=[$c_T(t_0)$, $c_T(t_1)$, … , $c_T(t_m)$]^T are the PET measurements at the sampling time, θ=[P_0, P_1, P_2, P_3]^T are the parameters to be estimated and X is the coefficient matrix. The initial guess of a_v is needed to calculate the dual-input function in the third and fourth terms of eq. (8). The value used in this study is 0.8 as well. The Patlak-D-I-LLS solution for θ is

$$\hat{\theta}_{P-D-I-LLS} = \left(X^T X\right)^{-1} X^T y \quad (10)$$

where $\hat{\theta}_{P-D-I-LLS}$ represents the estimated θ in this Patlak-D-I-LLS step.

The second step estimation results would be used as the initial values of the third step estimation aiming to refine the results by Patlak-D-I-LLS. Substitute all the dual-input function terms in eq. (7) with eq. (5), then

$$c_T^{''}(t) = P_0 * c_a^{''}(t) + P_1 * c_a^{'}(t) + \hat{K}P_2 * c_a(t) + a_v(\hat{P}_0(c_v^{''}(t) - c_a^{''}(t)) + \hat{P}_1(c_v^{'}(t) - c_a^{'}(t)) + \hat{K}\hat{P}_2(c_v(t) - c_a(t))) - P_2 * c_T^{'}(t) \quad (11)$$

where $\hat{K}$ is the estimate in step one, $\hat{P}_0, \hat{P}_1, \hat{P}_2$ represent the most updated estimates. Take the Laplace transform of eq. (11) with the assumption that the initial conditions were all zeros, whiten the correlated equation errors with an autoregressive filter $s(s + \hat{P}_2)$, and then take the inverse Laplace transform, the time domain output function is

$$c_T(t) - \hat{P}_2\psi_1 \otimes c_T(t) = P_0\left(c_a(t) - \hat{P}_2\psi_1 \otimes c_a(t)\right) + P_1\psi_1 \otimes c_a(t) + P_2\left(\hat{K}\psi_2 \otimes c_a(t) - \psi_1 \otimes c_T(t)\right) + a_v\left(\hat{P}_0(c_v(t) - c_a(t)) + (\hat{P}_1 - \hat{P}_0\hat{P}_2)\psi_1 \otimes (c_v(t) - c_a(t)) + \hat{K}\hat{P}_2\psi_2 \otimes (c_v(t) - c_a(t))\right) \quad (12)$$

where

$$\psi_1 = e^{-\hat{P}_2 t}$$
$$\psi_2 = \frac{1}{\hat{P}_2}(1 - e^{-\hat{P}_2 t})$$

Digitalize eq. (12) at the sampling time, then

$$r = Z\theta + \zeta \quad (13)$$

where r is the filtered PET measurements at the sampling time, ζ is the filtered equation errors, θ=[P_0, P_1, P_2, a_v]^T are the parameters to be estimated, and Z is the coefficient matrix. The solution of the Patlak-D-I-GLLS is

$$\hat{\theta}_{P-D-I-GLLS} = \left(Z^T Z\right)^{-1} Z^T r \quad (14)$$

where $\hat{\theta}_{P-D-I-GLLS}$ represents the estimated θ in Patlak-D-I-GLLS sense. Eq. (14) would be repeated until the termination criteria are satisfied. In this study, the termination criteria are either maximum iteration of twenty was reached or the Euclidean norm of difference of parameter estimates between two successive iterations was less than 0.0001. In the fourth step estimation, Parameter K would be estimated by Patlak method with the estimated a_v in step three to calculate the dual-input function.

2.5 Simulation studies.

Computer simulation was conducted to both NLS and Patlak-D-I-GLLS algorithms. There were two sets of computer simulated data including one representing HCC with two image-derived dual-input functions acquired from two patients recruited in this study. The sampling sequences were the same as those of clinical data acquisition. A pseudorandom number generator was used to generate the Gaussian noise added to the calculated tissue TAC (TTAC) and the noise level (the proportional constant in the variance of the generated noise) was set to 0.1, 0.5 and 1.0 respectively. The estimation accuracy and reliability were evaluated by *bias* and *CV* respectively.

3. RESULTS AND CONCLUSION

In Patlak-NLS fitting, the estimation of LHMRAct (the forward clearance K) is by linear Gjedde-Patlak analysis, it is generally accepted that the fitting results are very robust. The estimation reliability in terms of the *CV* of another two macroparameters is satisfactory as well. The *CVs* of all the macroparameters are generally less than the *CV* of the most reliably estimated K_1 by NLS method. Therefore, the model rate constant parameters K_1, k_2, k_3 could be much more reliably estimated by the proposed Patlak-NLS technique.

The fitting results of a_v and *HBV* by NLS and Patlak-NLS methods were summarized in Table 1. As could be seen, the two sets of estimated a_v values are approximately the same except region 8. For the eight nontumor liver tissue regions, the estimated a_v values are 0.8174 ± 0.0898 and 0.7935 ± 0.1040 by Patlak-NLS and NLS methods respectively. The estimation of a_v by Patlak-NLS is reliable, since half of the *CVs* are less than 10% and most of them are less than 20%. Majority *CVs* of the estimated a_v by Patlak-NLS are less than those by NLS, and the estimated a_v of region 10 is considerably more reliable. All these findings suggest that Patlak-NLS method could provide accurate and reliable fitting results for the potential HCC indicator: Parameter a_v. The estimates of *HBV* by the two methods are nearly the same except regions 1 and 8. The estimation of *HBV* tends to be slightly less reliable than that by NLS in some cases. However, the estimation of *HBV* of region 10 is significantly more reliable, the average *CV* is a little bit smaller and all the *CVs* of the estimated *HBV* are generally acceptable. The fitted curves of the generated TACs of HCC and nontumor liver tissue ROIs by using patlak-NLS and NLS methods were demonstrated in Fig. 2. As shown in Fig. 2, the two fitted curves for HCC by the two methods are identical to each other; for the nontumor liver tissue data, the curve fitted by Patlak-NLS demonstrates better results.

Table 1 The parameter estimates of clinical datasets by NLS and Patlak-NLS methods. CV_a and CV_H are the *CVs* of the estimated a_v and *HBV* respectively.

	NLS				Patlak-NLS			
	a_v	CV_a(%)	*HBV*	CV_H(%)	a_v	CV_a(%)	*HBV*	CV_H(%)
1	0.9128	6.62	0.0965	47.91	0.9110	7.85	0.0644	69.01
2	0.7002	19.72	0.0419	65.81	0.7175	19.25	0.0430	71.75
3	0.8634	8.46	0.0547	54.03	0.8897	7.57	0.0538	59.22
4	0.7174	3.30	0.3277	5.50	0.7127	5.49	0.3101	9.26
5	0.6744	8.59	0.2948	13.08	0.7238	8.65	0.3144	14.81
6	0.8989	4.20	0.4749	11.50	0.8983	3.72	0.4735	9.23
7*	0.3632	65.46	0.1758	52.26	0.3756	67.39	0.2054	53.31
8	0.6987	16.32	0.0873	58.06	0.7937	14.02	0.1671	58.36
9	0.8819	12.55	0.0810	98.77	0.8929	10.04	0.0850	99.01
10*	0.5908	45.88	0.1602	76.07	0.5610	17.19	0.1411	35.60

**Regions 7 and 10 represent HCC.*

During the Patlak-NLS fitting procedure, the number of parameters to be estimated by the recursive NLS procedure is reduced, therefore, the fitting results are less affected by the initial guess and the computational time-complexity is considerably reduced.

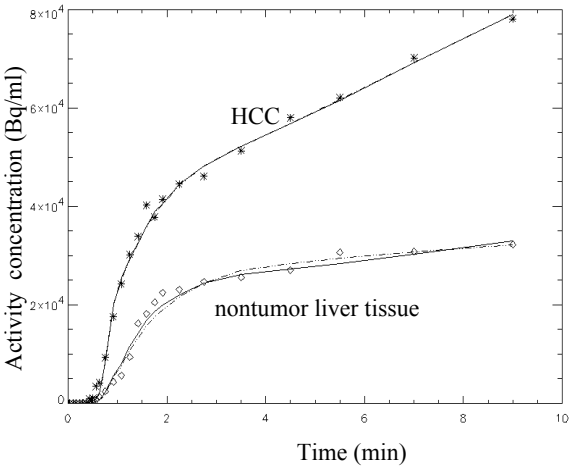

Fig. 2. The fitting results of the generated TACs of HCC and nontumor liver tissue ROIs from one clinical dataset. Asterisk represents HCC data, while diamond represents nontumor liver tissue data. The fitted curves by using patlak-NLS and NLS methods were drawn by solid and dash dot dot lines respectively.

The Patlak-D-I-GLLS method was tested by computer simulation. The estimation results of the mean values, *biases*, and *CVs* of K_1-k_3, *HBV*, a_v and K calculated from 200 simulation runs by NLS and Patlak-D-I-GLLS were presented in Table 2. As seen in Table 2, the estimation quality in terms of *CV* and *bias* of the estimated a_v and *HBV* by Patlak-D-I-GLLS is comparable with that by NLS method. Parameter a_v could be reliably and accurately identified by using Patlak-D-I-GLLS. More reliable estimates of K could be provided by Patlak-D-I-GLLS than by NLS and the rate constant parameters K_1-k_3 could be considerably more reliably estimated as well. The estimation accuracy of K and K_1-k_3 is satisfactory. The accuracy of the estimated K_1-k_3 is less sensitive to the noise level and the accuracy of the two HCC indicators: a_v and LHMRAct (the forward clearance K) is not sensitive to the noise level at all. Furthermore, since all of the parameters could be estimated by linear fitting and calculated analytically, the Patlak-D-I-GLLS procedure is significantly faster. Therefore, Patlak-D-I-GLLS is particularly valuable for noisy clinical environments.

Two novel parameter estimation techniques for dual-input ^{11}C-acetate kinetic model with dynamic PET images were presented in this study. When compared with NLS method, the computational time-complexity of Patlak-NLS technique is reduced, the fitting results are less affected by the initial guess and more reliable estimates could be provided. Patlak-D-I-GLLS algorithm could generally identify all the parameters more reliably including the parameter in the dual-input function and the fitting procedure is significantly faster. The estimation accuracy and reliability of the two HCC indicators are satisfactory by both presented methods. Therefore, the proposed approaches suggest better ways for the evaluation of HCC, and are potentially applicable for other dual-input biomedical systems.

Table 2 Estimation results of K_1-k_3, HBV, a_v and K from two sets of simulation. The second set of data represent HCC. The estimated parameters represent their mean values. The mean values, *biases* (percentage value) and *CVs* were calculated from 200 simulation runs. "Pat-G" is the abbreviation of "Patlak-D-I-GLLS".

Method	K_1	$bias_1$	CV_1(%)	k_2	$bias_2$	CV_2(%)	k_3	$bias_3$	CV_3(%)	HBV	$bias_H$	CV_H(%)	a_v	$bias_a$	CV_a(%)	K	$bias_K$	CV_K(%)
$P_{1\text{-true}}$	0.65	---	---	0.40	---	---	0.15	---	---	0.30	---	---	0.72	---	---	0.1773	---	---
Noise level α=0.1																		
NLS	0.6504	0.06	0.70	0.4004	0.09	1.49	0.1500	0.03	1.41	0.3001	0.03	1.99	0.7204	0.05	1.11	0.1772	0.03	0.55
Pat-G	0.6484	0.24	0.51	0.4063	1.58	0.84	0.1560	3.98	0.78	0.3048	1.61	1.81	0.7214	0.20	1.14	0.1787	0.83	0.33
Noise level α=0.5																		
NLS	0.6511	0.17	3.61	0.4012	0.31	7.59	0.1495	0.35	7.04	0.3009	0.28	9.97	0.7208	0.11	5.46	0.1767	0.33	2.78
Pat-G	0.6494	0.10	2.61	0.4069	1.72	4.16	0.1557	3.78	3.85	0.3035	1.17	9.15	0.7161	0.54	5.92	0.1784	0.65	1.63
Noise level α=1																		
NLS	0.6513	0.20	7.45	0.4022	0.56	15.50	0.1483	1.16	14.28	0.3027	0.89	19.69	0.7194	0.08	10.82	0.1753	1.12	5.88
Pat-G	0.6479	0.32	5.67	0.4064	1.60	10.01	0.1555	3.68	7.94	0.3061	2.02	17.81	0.7142	0.81	11.81	0.1779	0.38	3.14
$P_{2\text{-true}}$	1.30	---	---	0.35	---	---	0.10	---	---	0.30	---	---	0.36	---	---	0.2889	---	---
Noise level α=0.1																		
NLS	1.3006	0.04	1.30	0.3501	0.04	2.15	0.0999	0.13	1.70	0.3008	0.27	5.04	0.3612	0.33	8.18	0.2887	0.08	0.82
Pat-G	1.2800	1.54	0.96	0.3412	2.52	1.39	0.0974	2.59	0.87	0.3209	6.97	5.82	0.3629	0.80	8.88	0.2772	4.04	0.50
Noise level α=0.5																		
NLS	1.2940	0.46	6.27	0.3478	0.64	10.51	0.0987	1.34	8.66	0.3111	3.69	26.20	0.3583	0.47	40.59	0.2860	1.02	4.34
Pat-G	1.2743	1.98	4.71	0.3400	2.86	6.73	0.0974	2.62	4.38	0.3321	10.71	28.08	0.3611	0.31	42.44	0.2766	4.25	2.47
Noise level α=1																		
NLS	1.2829	1.31	11.12	0.3453	1.33	19.23	0.0970	2.99	17.57	0.3384	12.81	49.72	0.3590	0.27	70.14	0.2808	2.80	9.48
Pat-G	1.2555	3.42	10.43	0.3354	4.16	15.05	0.0976	2.43	9.06	0.3525	17.50	49.88	0.3504	2.68	84.23	0.2754	4.65	4.91

ACKNOWLEDGEMENT

This work was supported by the studentship of the Hong Kong Polytechnic University, and partially by UGC and ARC grants.

REFERENCES

Carson, R. E., S. C. Huang, and M. V. Green (1986). Weighted integration method for local cerebral blood flow measurements with positron emission tomography. *Journal of Cerebral Blood Flow and Metabolism*, **vol. 6**, pp. 245-258.

Chen, K., M. Lawson, E. Reiman, A. Cooper, D. Feng, S. C. Huang, D. Bandy, D. Ho, L. Yun, and A. Palant (1998). Generalized linear least squares method for fast generation of myocardial blood flow parametric images with N-13 Ammonia PET. *IEEE Transactions on Medical Imaging*, **vol. 17, no. 2**, pp. 236-243.

Chen, S. and D. Feng (2004). Non-invasive quantification of the differential portal and arterial contribution to the liver blood supply from PET measurements using ^{11}C-acetate kinetic model. *IEEE Transactions on Biomedical Engineering*, **vol. 51, no. 9**, pp. 1579-1585.

Chen, S., C. Ho, D. Feng, and Z. Chi (2004). Tracer kinetic modeling of ^{11}C-acetate applied in the liver with positron emission tomography. *IEEE Transactions on Medical Imaging*, **vol. 23, no. 4**, pp. 426-432.

Feng, D., S. C. Huang, Z. Wang, and D. Ho (1996). An unbiased parametric imaging algorithm for nonuniformly sampled biomedical system parameter estimation. *IEEE Transactions on Medical Imaging*, **vol. 15, no. 4**, pp. 512-518.

Ho, C.-L., S. Yu, and D. Yeung (2003). ^{11}C-acetate PET imaging in hepatocellular carcinoma and other liver masses. *Journal of Nuclear Medicine*, **vol. 44, no. 2**, pp. 213-221.

Huang, S. C., R. E. Carson, and M. E. Phelps (1982). Measurement of local blood flow and distribution volume with short-lived isotopes: A general input technique. *Journal of Cerebral Blood Flow and Metabolism*, **vol. 2**, pp. 99-108.

Munk, O. L., L. Bass, K. Roelsgaard, D. Bender, S. B. Hansen, and S. Keiding (2001). Liver kinetics of glucose analogs measured in pigs by PET: Importance of dual-input blood sampling. *Journal of Nuclear Medicine*, **vol. 42, no. 5**, pp. 795-801.

Patlak, C. S., R. G. Blasberg, and J. D. Fenstermacher (1983). Graphical evaluation of blood-to-brain transfer constants from multiple-time uptake data. *Journal of Cerebral Blood Flow and Metabolism*, **vol. 3, no. 1**, pp. 1-7.